Recent results on vector boson production in association with jets with the CMS detector

Tom Cornelis, for the CMS collaboration

Department of Elementary Particle Physics, University of Antwerp,
Groenenborgerlaan 171, 2020 Antwerp, Belgium

The production of weak vector bosons in association with jets and their properties are intensively studied using proton-proton collision data collected with the CMS detector. In this proceedings, we will show the cross section measurement of the electroweak production of a Z boson in association with 2 jets at $\sqrt{s} = 8$ TeV, including a new data-driven approach and studies on the hadronic activity in the region between the two tagging jets. The azimuthal correlations and event shapes in Z + jets events at $\sqrt{s} = 7$ TeV are also presented.

1. Azimuthal correlations and event shapes in Z plus jet events

Azimuthal correlations in Z plus at least one jet events were studied [1] in pp collisions at $\sqrt{s} = 7$ TeV, using 5 fb^{-1} of data recorded with the CMS detector [2]. Events were selected by requiring an oppositely charged electron or muon pair with an invariant mass within a window of 20 GeV around the Z boson mass. Both leptons satisfy $p_T > 20$ GeV and $|\eta| < 2.4$ and fulfill quality and isolation criteria. Jets with $p_T > 50$ GeV and $|\eta| < 2.5$ were used, clustered using the anti-k_T algorithm with size parameter of 0.5.

1.1. Azimuthal angles

Figure 1 shows the azimuthal angle between the Z boson and the leading jet, either for all Z bosons or in a subset of events with $p_T^Z > 150$ GeV, a region which is critical in searches for new phenomena. The results agree within uncertainties with the MadGraph [3] prediction. In $Z+ \geq 1$ jet events, the Sherpa [4] prediction is about 10% too low whereas Powheg [5, 6, 7, 8] overestimates the distribution by about 10%. The Z boson and leading jet are completely correlated for $N_{jets} = 1$, as $\Delta\phi(Z, j_1)$ tends to π. If $\Delta\phi(Z, j_1) < \frac{\pi}{2}$, the leading jet and Z boson are in the same hemisphere and therefore balanced by subleading jets in the opposite hemisphere which results in a more isotropic $\Delta\phi(Z, j_1)$ distribution for larger inclusive jet multiplicities.

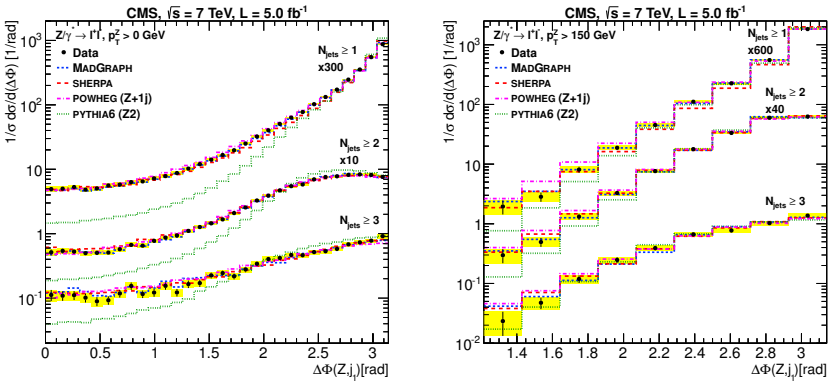

Fig. 1. Normalized $\Delta\phi(Z, j_1)$ distributions categorized as a function of jet multiplicity. The yellow band shows the sum of statistical and systematic errors on the data. *(left)* All p_T^Z *(right)* $p_T^Z > 150$ GeV.

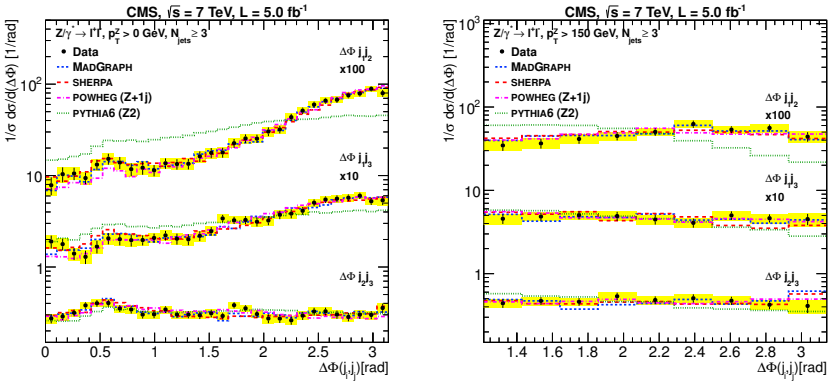

Fig. 2. Normalized $\Delta\phi(j_i, j_j)$ distributions for the inclusive $N_{jets} > 3$ multiplicity bin. The yellow band shows the sum of statistical and systematic errors on the data. *(left)* All p_T^Z *(right)* $p_T^Z > 150$ GeV.

There is good agreement between MADGRAPH, SHERPA and PYTHIA [9] predictions, and the data for the azimuthal angles among the three leading jets, shown in Figure 2. For higher p_T^Z, these angles decorrelate.

1.2. Transverse thrust

The properties of Z plus jet events have also been studied using the transverse thrust τ_{T}, defined as $\tau_{\mathrm{T}} \equiv 1 - \max_{\vec{n}_\tau} \frac{\sum_i |\vec{p}_{\mathrm{T},i} \cdot \vec{n}_\tau|}{\sum_i p_{\mathrm{T},i}}$ where the sum

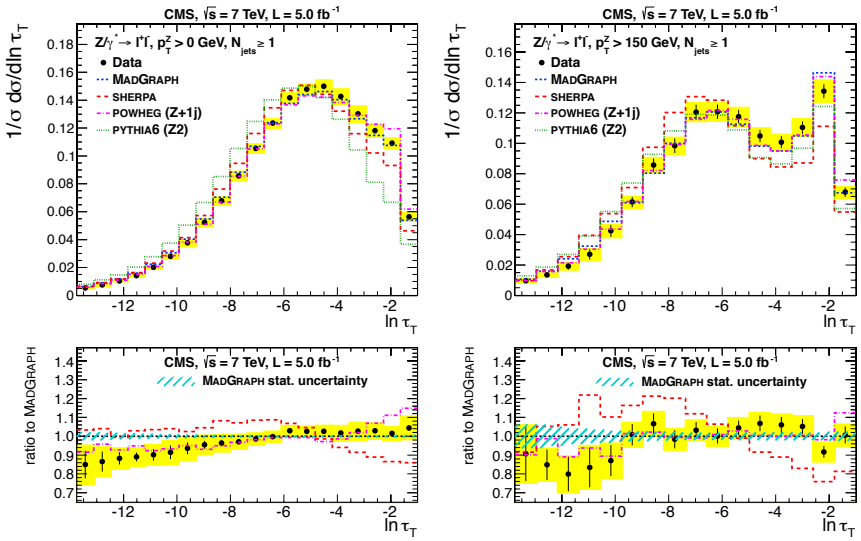

Fig. 3. Normalized distributions in ln τ_{T} for Z plus at least 1 jet events for *(left)* all p_T^Z *(right)* $p_T^Z > 150$ GeV. The yellow band shows the sum of statistical and systematic errors on the data.

over i runs over the Z and each accepted jet in the event. The sum is maximized by the unit vector $\vec{n}_\tau$, called the thrust axis. In the limit of a perfectly balanced Z plus one jet event, τ_{T} tends to zero (ln $\tau_{\mathrm{T}} \to -\infty$). In the limit of a homogeneously distributed event, the transverse thrust reaches $1 - \frac{\pi}{2}$ (ln $\tau_{\mathrm{T}} \to -1$), its maximum possible value. The ln τ_{T} distribution is shown in Figure 3. The data is best described by POWHEG and MADGRAPH, except at large negative values for the transverse thrust where an overestimation by MADGRAPH is seen. PYTHIA and SHERPA have larger discrepancies and predict also too small values for ln τ_{T}. The peak at ln $\tau_{\mathrm{T}} \approx -2$ in the boosted region corresponds with events where the Z is balanced by two or more jets.

2. Electroweak production of Z + 2 jets

Although most Zjj events at the LHC are produced by Drell-Yan (DY) processes, the the same final state could also be created only by electroweak interactions. Three classes of diagrams, shown in Figure 4, contribute to the electroweak Zjj production: bremsstrahlung, vector boson fusion (VBF) processes and multi-peripheral. There is great interest in the study of the VBF diagram, which establishes a foundation for the more general study of VBF processes which include Higgs boson studies and supersymmetry

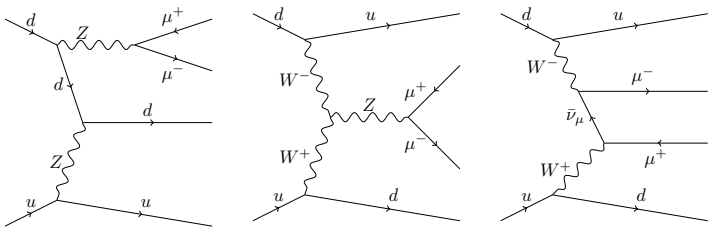

Fig. 4. Representative diagrams for the electroweak Zjj production processes.

searches. However, all three categories should be studied together, as large negative interference effects exists between the VBF process and the other two categories.

The pure electroweak cross section of a Z boson in association with two jets has already been measured with the CMS detector in pp collisions at $\sqrt{s} = 7$ TeV [10]. We will discuss now the first preliminary results using the $\sqrt{s} = 8$ TeV dataset (19.7 fb^{-1}) [11], which includes the addition of a data-driven method that models the DY background using γjj events.

Events are selected by requiring a muon or electron pair with opposite charge, in which both leptons satisfy a series of quality and isolation criteria, a transverse momentum of at least 20 GeV and $|\eta| < 2.4$. The Z bosons are reconstructed by taking events with a dilepton mass within the 15 GeV mass interval around the nominal Z boson mass. The two leading jets within $|\eta| < 4.7$ and exceeding $p_T^{j_1,j_2} > 50, 30$ GeV are selected as the tagging jets.

2.1. Cross section measurement

Because the signal is small compared with the main background, DY Zjj, a precise modeling of this background is necessary. However, the simulation is based on MadGraph and therefore lacks possible virtual corrections at higher order then the Born level. A first method, also used in the 7 TeV analysis, corrects the MadGraph simulation with dynamical k-factors derived from NLO predictions with mcfm for the dijet invariant mass and the $y^* = y_Z - 0.5(y_{j1} + y_{j2})$ variable. For the 8 TeV analysis, a data-driven approach is added. It is expected that the kinematics of dijet system in DY Zjj are similar to the dijet system in photon plus 2 jet events. A reweighting of the p_T of the photon to the p_T of the Z candidate is used to eliminate differences induced by specific γ or Z sample selections. Because the photon sample is at low p_T affected by multijet production and high trigger prescales, the p_T of the photon or Z is required to be larger than 50 GeV.

Both methods use multi variate analysis techniques. The signal cross

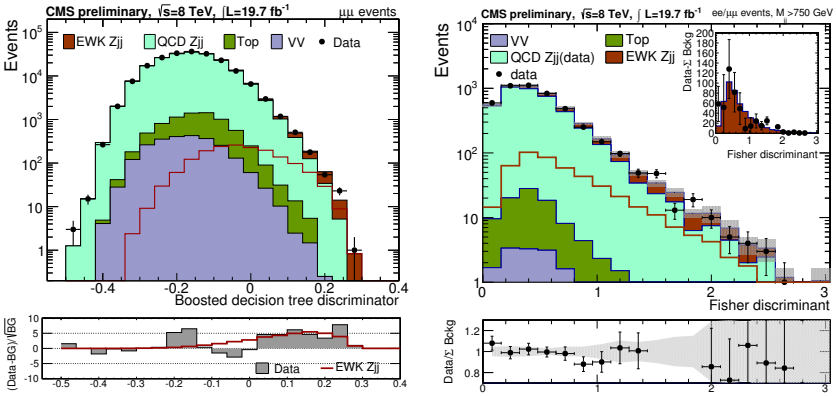

Fig. 5. Shape discriminators used for the signal cross section extraction *(left)* BDT using simulated background *(right)* dijet Fisher discriminator using data-driven background estimation

sections are extracted by fitting the output shapes for signal and background to the data (Figure 5). For the simulation based method, this is a boosted decision tree (BDT) built out of the following variables: the p_T of the tagging jets, the pseudorapidity separation between them, the invariant dijet mass, the y^* variable, the transverse momentum and rapidity of the dilepton system, the sum of the pseudorapidities of the two tagging jets and the difference between the azimuthal angles $(\phi_Z - \phi_{j1})$ and $(\phi_{j1} - \phi_{j2})$. The measured cross section with this method is $\sigma_{meas}^{EW\ \mu\mu jj} = 191 \pm 29\ (\text{stat}) \pm 39\ (\text{syst})$ fb. The cross section in the simulation based method is based only on the dimuon channel.

For the data-driven approach, a linear Fisher discriminant is constructed, only based on dijet kinematics: the pseudorapidity distance $\Delta\eta_{jj}$ between the two jets, the dijet invariant mass M_{jj} and the relative balance of the dijet system. The cross section, combining the dielectron and dimuon channels, is $\sigma_{meas}^{EW\ lljj} = 303 \pm 29\,(\text{stat}) \pm 57\,(\text{syst})$ fb.

Both methods are combined using the Best Linear Unbiased Estimator technique [12, 13] resulting in:

$$\sigma_{meas}^{EW\ lljj} = 226 \pm 26\,(\text{stat}) \pm 35\,(\text{syst})\ \text{fb}$$

which is in agreement with the theoretical NLO prediction of 239 pb computed with VBFNLO[14].

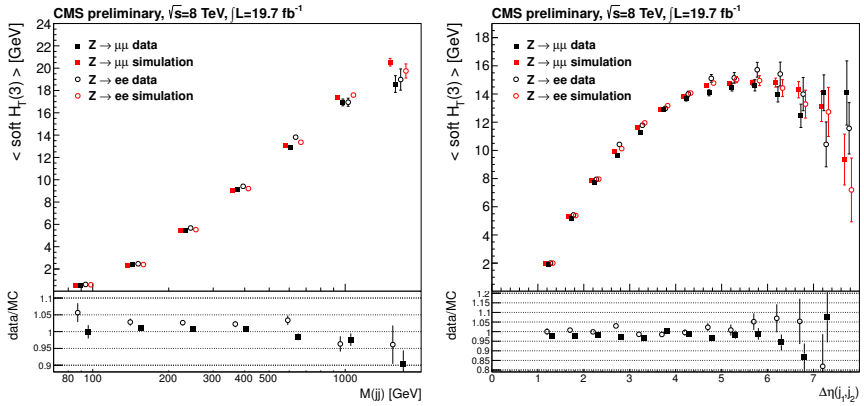

Fig. 6. Average H_T of the three leading soft track jets in the rapidity interval between the two leading jets with $p_T^{j_1,j_2} > 50, 30$ GeV in Zjj events versus *(left)* the dijet invariant mass *(right)* the pseudorapidity separation between the two tagging jets.

2.2. Central hadronic activity

Because there is no color flow between the two tagging jets in electroweak Zjj events, the hadronic activity between these jets is expected to be small. Although we do not use the hadronic activity to separate the EW Zjj from the backgrounds, studies have been done to test the agreement between data and simulation.

A first study makes use of soft track-jets. Tracks associated with the primary vertex and not associated with either of the two leptons or the two tagging jets are selected if they satisfy a high purity requirement and have a transverse momentum exceeding 300 MeV. These tracks are clustered into soft track jets with the anti-k_T algorithm with distance parameter of 0.5. This method gives us a collection of soft track-jets with energy as low as a few GeV which are not affected by the pileup.

In order to monitor the hadronic activity in the rapidity gap between the two tagging jets, only track-jets with pseudorapidity $\eta_{\rm min}^{\rm tag.jet} + 0.5 < \eta < \eta_{\rm max}^{\rm tag.jet} - 0.5$ are considered. The evolution of the average H_T as a function of the dijet invariant mass and the pseudorapidity separation between the two tagging jets is shown in Figure 6 and demonstrates a good agreement between data and simulation up to the highest regions of dijet invariant mass and pseudorapidity separation.

A second study is performed in a high purity region for which the dijet invariant mass is greater than 1250 GeV. This study makes use of jets with a

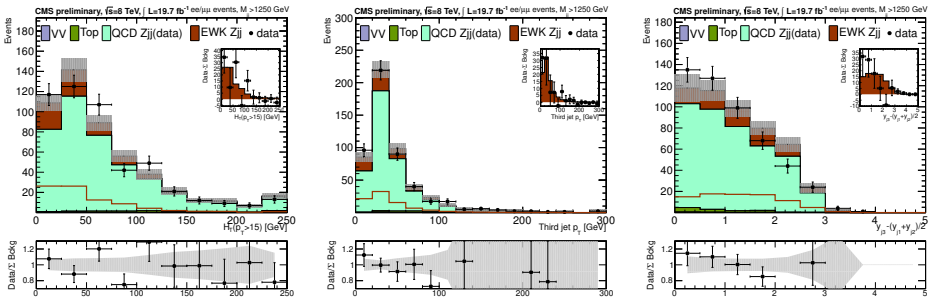

Fig. 7. Control distributions for the hadronic activity for events with $M_{jj} > 1250$ GeV *(left)* scalar sum of all jets with $p_T > 15$ GeV found in the pseudorapidity distance between the tagging jets *(middle)* p_T of the third jet *(right)* $y^*_{j_3}$

.

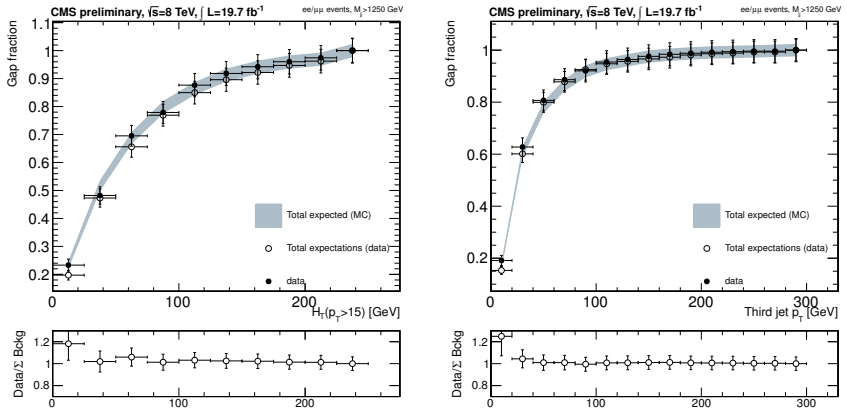

Fig. 8. Gap fraction versus *(left)* the scalar sum of the p_T of all jets *(right)* the p_T of the third jet.

$p_T > 15$ GeV, found in the pseudorapidity distance between the two tagging jets. The background prediction is modeled from the photon control sample. Figure 7 shows the scalar sum H_T of the p_T of these jets, the transverse momentum of the third jet, and its pseudorapidity measured in the dijet rest frame, which is slightly more central than expected. These distributions could be used to compute the efficiency of a hadronic veto either based on the transverse momentum of the third jet or on the H_T variable, as shown in Figure 8. The gap fraction corresponds to the fraction of events for which the tested variable does not exceed a given threshold and is calculated for data, simulation and the data-driven prediction.

3. Other results on vector boson production in association with jets

Besides the two analyses presented above, many other important benchmarks are recently achieved in V+jet studies using 7 TeV data. Recent results could be found on rapidity measurements in Z/γ plus jet events [15] and the study of double parton scattering in W plus 2 jet events [16]. Also the production of vector bosons in association with heavy flavor jets is studied, with measeruments which include the cross section of the production of Z plus one or two b jets [17, 19], the cross section and angular correlations for associated production of a Z boson with a b hadron [18], the cross section for W in association with 2 b jets [20], and the measurement of associated W plus charm production [21].

References

[1] CMS Collaboration, Phys. Lett. B **722**, 238 (2013).

[2] CMS Collaboration, J. Inst. **3**, S08004 (2008).

[3] J. Alwall *et al.*, J. High Energy Phys. **06**, 128 (2011).

[4] T. Gleisberg *et al.*, J. High Energy Phys. **02**, 007 (2009).

[5] P. Nason, J. High Energy Phys. **11**, 040 (2004).

[6] S. Frixione, P. Nason, and C. Oleari, J. High Energy Phys. **11**, 070 (2007).

[7] S. Alioli *et al.*, J. High Energy Phys. **06**, 043 (2010).

[8] S. Alioli *et al.*, J. High Energy Phys. **01**, 095 (2011).

[9] T. Sjostrand, S. Mrenna, and P.Z. Skands, J. High Energy Phys. **05**, 026 (2006).

[10] CMS Collaboration, J. High Energy Phys. **10**, 101 (2013).

[11] CMS Collaboration, CMS-PAS-FSQ-12-035 (2013).

[12] L. Lyons, D. Gibaut, and P. Clifford, Nucl. Instrum. Meth. A **270**, 110 (1988).

[13] L. Lyons, A.J. Martin, and D.H. Saxon, Phys. Rev. D **41**, 982 (1990).

[14] K. Arnold *et al.*, Comput. Phys. Commun. **180**, 1661 (2009).

[15] CMS Collaboration, CMS-PAS-SMP-12-004 (2013).

[16] CMS Collaboration, CMS-PAS-FSQ-12-028 (2013).

[17] CMS Collaboration, CMS-PAS-EWK-11-012 (2012).

[18] CMS Collaboration, CMS-PAS-EWK-11-015 (2013).

[19] CMS Collaboration, CMS-PAS-SMP-13-004 (2013).

[20] CMS Collaboration, CMS-PAS-SMP-12-026 (2013).

[21] CMS Collaboration, CMS-PAS-SMP-12-002 (2013).